Structural, magnetic and transport properties of $SmBa_xSr_{1-x}Co_2O_{5+\delta}$ ($0.1 \leq x \leq 0.5$)

Cite as: AIP Advances **8**, 105316 (2018); https://doi.org/10.1063/1.5045492
Submitted: 20 June 2018 . Accepted: 07 September 2018 . Published Online: 12 October 2018

S. N. Qadri, S. B. Qadri, D. H. Wu, R. Goswami, and M. Osofsky

Structural, magnetic and transport properties of $SmBa_xSr_{1-x}Co_2O_{5+\delta}$ ($0.1 \leq x \leq 0.5$)

S. N. Qadri, S. B. Qadri,[a] D. H. Wu, R. Goswami, and M. Osofsky
U. S. Naval Research Laboratory, Washington, D.C. 20375, USA

(Received 20 June 2018; accepted 7 September 2018; published online 12 October 2018)

The structural, transport, and magnetic properties of bulk $SmBa_xSr_{1-x}Co_2O_{5+\delta}$ samples were investigated as a function of Ba content. At room temperature the magnetization was observed to increase as a function of decreasing Ba composition. As the samples were cooled below room temperature, a ferromagnetic transition was observed for $0.1 \leq x \leq 0.5$ with the Curie temperatures showing a linear dependence on the Ba-composition. Transport measurements showed that resistivity values increased with decreasing temperature indicating a semiconducting-like behavior.
https://doi.org/10.1063/1.5045492

I. INTRODUCTION

Since the discovery of colossal magneto-resistance (CMR) behavior consisting of coincident paramagnet to ferromagnet/antiferromagnet and insulator-to-metal phase transitions interest in magnetic oxide materials doped with 3d transition metals has increased significantly. More recently, such oxide materials also have attracted much attention because of their possible multiferroic properties and the possibility of them being room temperature magnetic semiconductors. These materials have many potential practical applications, such as data storage devices, read head devices, sensor technology, and magnetic refrigeration.[1–3] After the initial studies of CMR in the manganates, other materials, such as the cobalt oxides, attracted great interest.[4–9] Among the cobalt oxides, $La_{1-x}Sr_xCoO_3$ has been of interest because of its magnetoresistance properties in high magnetic fields. In addition, $La_{1-x}Sr_xMnO_{3+\delta}$ (LSMO) and $La_{1-x}Sr_xCoO_{3-\delta}$ (LSCO) have been the focus of attention for their potential applications in solid oxide fuel cell applications because of their structural stability at higher temperatures. Similarly, $LnSr_{0.5}Ba_{0.5}Co_2O_{5+\delta}$ with Ln=Pr, Sm, and Gd have been investigated as electrode materials for solid oxide fuel cells (SOFC).[10–13] Even though these materials are excellent materials for SOFC applications, they have equally important magnetic and electrical properties. Specially, the oxygen-deficient $LnBaCo_2O_{5+\delta}$ where Ln=Eu and Gd have shown R_0/R_H ratios greater than 10 where R_H, and R_0 are the resistances in a magnetic field and without field, respectively. These oxides have a double-layered perovskite "112" type structure. The structural and magnetic studies of $LnBaCo_2O_{5+\delta}$ (where Ln=Pr, Nd, Sm, Eu, Gd, Tb, Dy) showed metal-insulator transitions in the resistivity measurements in the range $310 \leq T_{MI} \leq 360$ K correlated with appearance of ferromagnetic component and is correlated to the $O_{5.5}$ stoichiometry.[14] The electrical conductivity of $SmBaCo_2O_5$ exhibited a metal–insulator transition at about 250 °C. It showed semiconductor behavior from room temperature to 250 °C and metallic conductivity above 250 °C.[15] The effect of adding Sr as a substitution for Ba in $GdBa_xSr_{1-x}Co_2O_{5+\delta}$ has been investigated for $0 \leq x \leq 1.0$ in terms electrical conductivity.[16] It was found that these samples exhibit an M_I transition around 200 °C and the transition becomes less pronounced with increasing Sr content. The increasing Sr content in $SmBa_xSr_{1-x}Co_2O_{5+\delta}$ samples was found to improve the electrical conductivity at room temperature and they all show metallic like conductivity at high temperature. Since, there were no

[a]Syed.qadri@nrl.navy.mil

electrical data was available at low temperatures, we investigated both their electrical and magnetic properties.

In this paper, we report on the electrical conductivity at low temperatures and magnetic properties of bulk $SmBa_xSr_{1-x}Co_2O_{5+\delta}$ samples as a function of Ba content both at room temperature and low temperatures. At room temperature the magnetization was observed to increase as a function of decreasing Ba composition. As the samples were cooled below room temperature, a ferromagnetic transition was observed for $0.1 \leq x \leq 0.5$ with the Curie temperatures showing an inverse linear dependence on the Ba-composition. Transport measurements showed that resistivity values increased with decreasing temperature indicating a semiconducting-like behavior. The results show the existence of paramagnetic-to-ferromagnetic transition in this system with Curie temperatures having a linear dependence on the Ba-composition at the same time their electrical conductivities show semiconductor-like behavior.

II. EXPERIMENTAL DETAILS

Samples of $SmBa_xSr_{1-x}Co_2O_{5+\delta}$ were prepared by solid state reaction of stoichiometric compositions of Sm_2O_3, $BaCO_3$, SrO, and Co_3O_4 that were pressed in a hydraulic press to form cylindrical disks with a one-cm diameter and a height of 2-3mm. After de-carbonation at 1000°C, the pellets were heated for 24 to 36 hours in air at 1000°C and subsequently slow cooled to room temperature. The X-ray diffraction scans were obtained using CuKα radiation from a Rigaku 18 kW rotating anode source and a powder diffractometer at room temperature. The scanning rate for 2θ was 1 degree/minute. Transmission electron microscopy (TEM) and high-resolution TEM (HRTEM) were used to characterize the microstructure using Phillips CM 30 and JEOL 2200-FX analytical transmission electron microscopes. TEM samples were prepared by transferring a few drops of alcohol containing fine powder to a carbon coated fine mesh Cu-grid. Fast-Fourier transforms (FFTs) were obtained from the experimental HRTEM images using Digitalmicrograph™ software. A fine probe (probe size: 0.5nm) Energy dispersive X-ray spectroscopy (EDS) in the scanning TEM mode was used to determine the elemental composition. Magnetic measurements were performed on a Digital Measurement Systems Technologies vibrating sample magnetometer (VSM). Thermal variations of the magnetization, M, versus magnetic field, H, and their hysteresis loops were measured using a Quantum Design SQUID magnetometer between 2 and 300K. In addition, M versus H loops for different compositions were obtained using the vibrating sample magnetometer. The electrical resistivity was measured using Quantum Design PPMS system with magnetic field on and with the field off.

III. RESULTS AND DISCUSSION

Figure 1 shows an overlay of XRD scans taken at room temperature for powder samples of $SmBa_xSr_{1-x}Co_2O_{5+\delta}$ for selected values of x using CuKα radiation. The peaks have been identified as those of the orthorhombic phase with a space group of Pmmm for x=1, 0.7 and 0.5 with their corresponding Miller indices. In addition, a few minor peaks are present in the diffraction scans that can be indexed based on a super cell similar to the ones reported in the literature.[13,14] However, the x-ray diffraction patterns for x=0.3 and x=0.1 are indexed based on a tetragonal unit cell having a space group of P4/mmm. The lattice parameters obtained after a least squares refinements are listed in Table I along with unit cell volumes. In addition, the lattice parameters for the x=0 sample which has a different space group, Pnma, are listed in Table I. The crystallite sizes were determined using Halder-Wagner method and are given in Table I. The crystallite sizes ranged between 35 to 46 nm. In general, the unit cell lattice parameters and their unit cell volumes show a decreasing linear trend with increasing Sr-content or decreasing Ba-content.

We performed high resolution transmission electron microscopy (HRTEM) on Sm $Ba_xSr_{1-x}Co_2O_{5+\delta}$ for the x = 0.3 and 0.5 samples to investigate the microstructure as well as the super cell formation. Both samples show the existence of super cell structure consistent with the XRD observations. Fig. 2(a) is the HRTEM image for the x=0.3 sample close to the [110] zone showing that the lattice spacing of the (001) plane is approximately 0.77nm. In few cases, Fig. 2b,

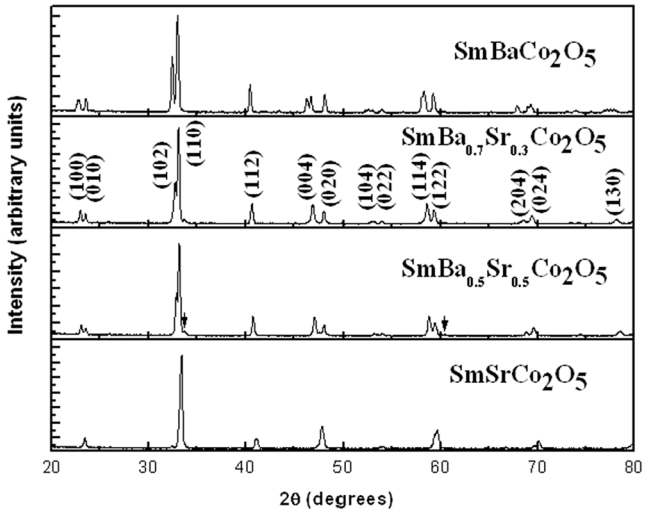

FIG. 1. An overlay of XRD scans of $SmBa_xSr_{1-x}Co_2O_{5+\delta}$ for x = 0.0, 0.5, 0.7, and 1.0 showing orthorhombic phases.

the (001) spacing was observed to be double. For x =0.5, the microstructure looks to be similar to that of x =0.3. Fig. 2(c) is the HRTEM for the x= 0.5 sample close to the [100] zone showing that the (001) lattice spacing is approximately 0.77nm that is observed in most parts of the sample. In a few areas we could observe the (001) spacing to be twice and three times the original spacing. The variation of the oxygen content of the structure and a possible ordering between oxygen and vacancies in the samarium layer results in the formation of supercell. Such ordering has also been reported in other lanthanides perovskite structures.[14] Energy Dispersive x-ray spectroscopy (EDS) data were also obtained from different areas of both samples to obtain the elemental ratios. Fig. 2(d) is the EDS spectrum for the x=0.5 sample showing the ratio of Sm:Ba:Sr:Co to be 0.57:0.3:0.25:1, which is close to the stoichiometric ratio.

The magnetic data obtained on the VSM showed paramagnetic behavior for all the samples at room temperature. The slope (M/H) showed a linear dependence on Ba composition with the

TABLE I. Lattice Parameters, Space Groups and Crystallite sizes versus compositions.

Composition	Phases	Lattice Parameters (Å)	Volume (Å^3)	Crystallite Size (nm)
$SmBaCo_2O_5$	Pmmm	a=3.886(0.015) b=3.905(0.003) c=7.574(0.011)	114.90	35.5
$SmBa_{0.8}Sr_{0.2}Co_2O_5$	Pmmm	a=3.877(0.015) b=3789(0.003) c=7.751(0.011)	113.86	40.1
$SmBa_{0.7}Sr_{0.3}Co_2O_5$	Pmmm	a=3.870(0.038) b=3.788(0.001) c=7.734(0.003)	113.39	35.0
$SmBa_{0.5}Sr_{0.5}Co_2O_5$	Pmmm	a=3.863(0.038) b=3.787(0.001) c=7.721(0.003)	112.95	32.0
$SmBa_{0.3}Sr_{0.7}Co_2O_5$	P4/mmm	a=3.817(0.004) c=7.696(0.041)	112.33	35.0
$SmBa_{0.1}Sr_{0.9}Co_2O_5$	P4/mmm	a=3.800(0.003) c=7.696(0.007)	111.13	40.5
$SmSrCo_2O_5$	Pnma	a=5.371(0.015) b=7.578(0.035) c=5.400(0.015)	219.83	46.1

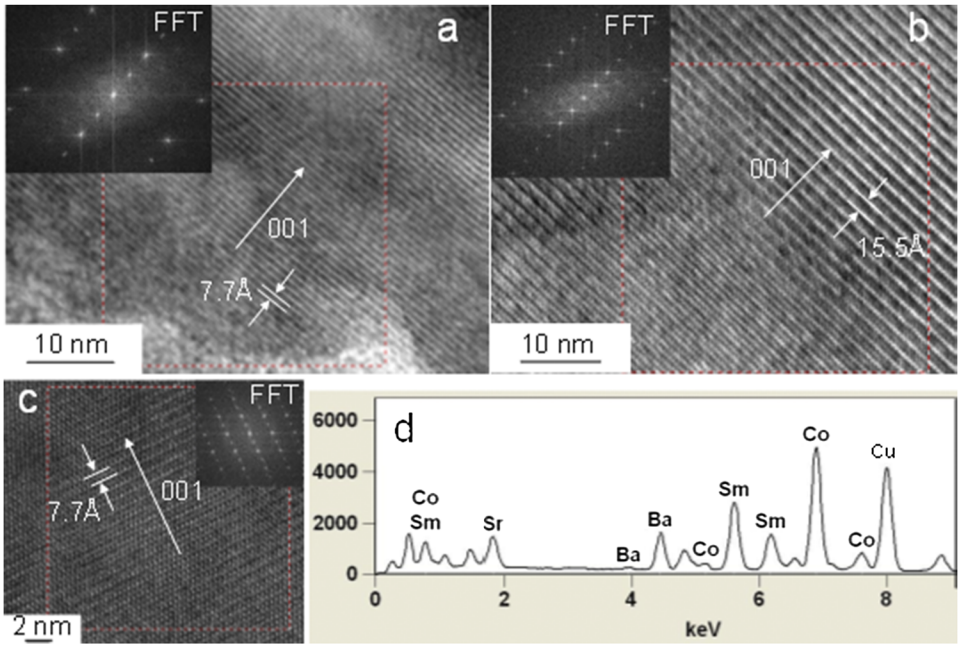

FIG. 2. (a) HRTEM for x=0.3 sample close to [110] zone (b) the doubling of thy (001) spacing (c) HRTEM for x=0.5 sample close to [100] zone (d) EDS spectrum for x=0.5 sample showing the stoichiometry ratio of Sm:Ba:Sr:Co.

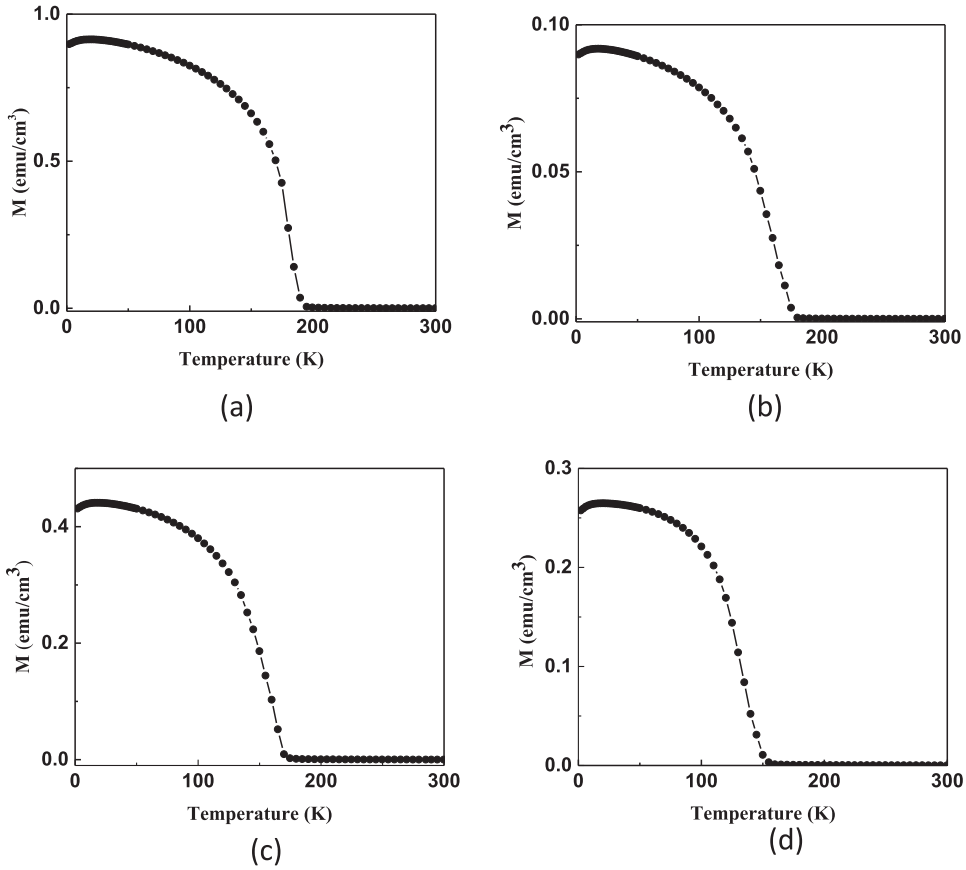

FIG. 3. M versus T (K) for (a) $SmBa_{0.1}Sr_{0.9}Co_2O_{5+\delta}$, (b) $SmBa_{0.2}Sr_{0.8}Co_2O_{5+\delta}$ (c) $SmBa_{0.3}Sr_{0.7}Co_2O_{5+\delta}$, and (d) $SmBa_{0.5}Sr_{0.5}Co_2O_{5+\delta}$.

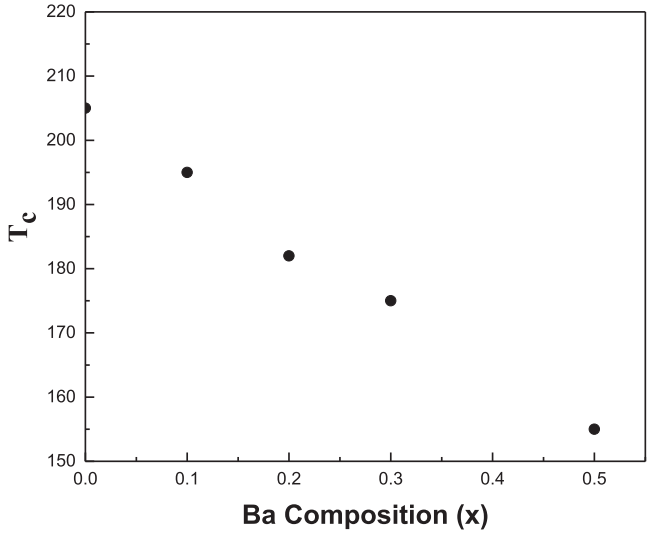

FIG. 4. T_c versus Ba composition (x).

magnetization decreasing with increasing Ba content. Figures 3a–3d show the M versus T data collected in a field-cooled cycle with a magnetic field of 10 G for the (a) $SmBa_{0.1}Sr_{0.9}Co_2O_{5+\delta}$ (b) $SmBa_{0.2}Sr_{0.8}Co_2O_{5+\delta}$, (c) $SmBa_{0.3}Sr_{0.7}Co_2O_{5+\delta}$, and (d) $SmBa_{0.5}Sr_{0.5}Co_2O_{5+\delta}$ samples. It is

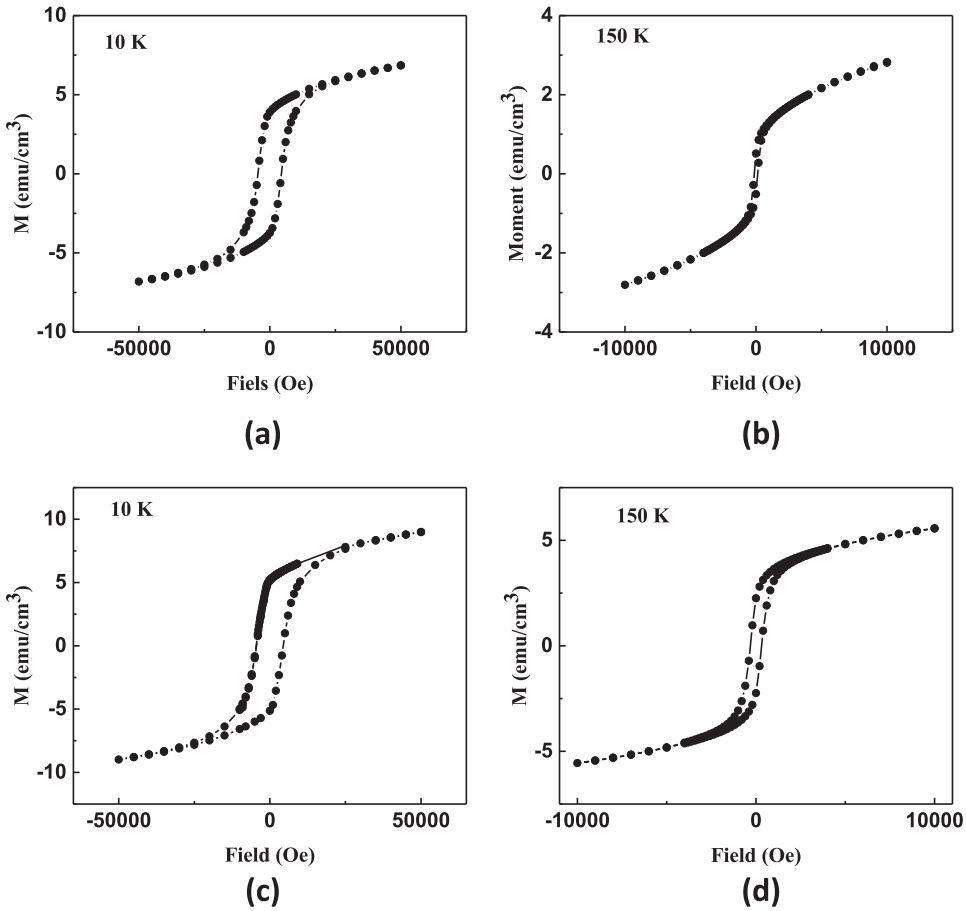

FIG. 5. M versus H hysteresis loops taken at 150 K and 10 K for $SmBa_{0.1}Sr_{0.9}Co_2O_{5+\delta}$ and $SmBa_{0.3}Sr_{0.7}Co_2O_{5+\delta}$.

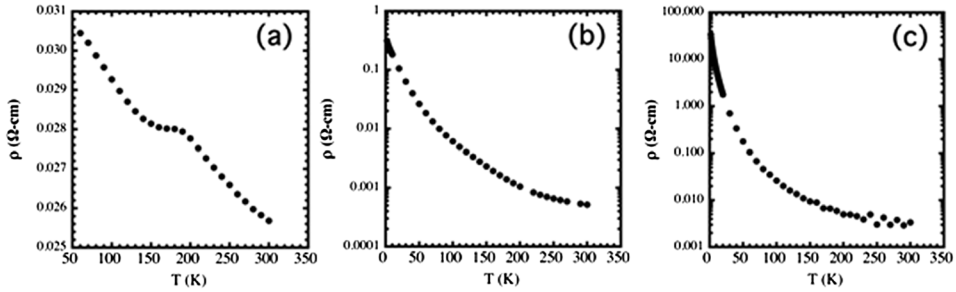

FIG. 6. R versus T (K) for (a) $SmBa_{0.1}Sr_{0.9}Co_2O_{5+\delta}$, (b) $SmBa_{0.3}Sr_{0.7}Co_2O_{5+\delta}$ (c) $SmBa_{0.5}Sr_{0.5}Co_2O_{5+\delta}$ showing decreasing resistance as a function of increasing temperature.

clear from this figure that these samples undergo ferromagnetic transitions as the temperature is lowered from room 300 K to 2 K. The Curie temperatures (T_c) determined for these samples show a linear decrease with increasing Ba composition (Figure 4). In order to investigate the ferromagnetic behavior of the samples, hysteresis loops were obtained for each sample at 150K and 10K. Figure 5 shows the hysteresis loops data taken at 150K and 10K for $SmBa_{0.1}Sr_{0.9}Co_2O_{5+\delta}$ and $SmBa_{0.3}Sr_{0.7}Co_2O_{5+\delta}$. Several factors such as oxidation state or the valence of Co, the interatomic distances, and the oxygen content can affect the saturation magnetization and the coercive field.

Electrical resistivity data obtained between 300K and 2K is shown in Fig. 6 for the samples that showed ferromagnetism, namely those with $0.1 \leq x \leq 0.5$. All three sample's resistivity increased with decreasing temperature with the x=0.3 and 0.5 samples. The x=0.1 sample had a much gentler temperature dependence with a kink around the Curie temperature that is due to the reduction of spin flip scattering and has been observed in various ferromagnetic materials.[17–19] The behavior of these samples is consistent with metal-insulator transition observed in the electrical conductivity of $SmBaCo_2O_5$[20] where below 250 °C semiconductor-like behavior was observed. Arrhenius plots of these data show they do not have well defined energy gaps. The different segments of the data were fitted to $\rho=\rho_0\exp(T_0/T)$ which gave us a value of T_0=0.3 K for low temperature region and T=80 K for the high end of temperature for x=0.5 sample. In addition, these results are consistent with what was reported for the substitution of Sr for $GdBa_xSr_{1-x}Co_2O_{5+\delta}$ for $0 \leq x \leq 1.0$ resulted in the improvement of the electrical conductivity at room temperature and they all showed metallic like conductivity at high temperatures and below T_{MI} semiconductor-like behavior.[21] In contrast, we have shown that even below room temperature to 4K, they all exhibit semiconductor-like conductivity.

IV. CONCLUSIONS

In conclusion, bulk samples of $SmBa_xSr_{1-x}Co_2O_{5+\delta}$ have been prepared by solid-state reaction and shown to exhibit different phases as a function of varying composition. For $0.1 \leq x \leq 0.5$ an orthorhombic phase was observed showing a linear decrease in unit cell volume with increasing x value. The electrical resistance of the samples increased as the temperature was lowered from 300K to 2K suggesting a semiconductor-like behavior of these materials consistent with metal-insulator transition reported above room temperature. Magnetic measurements showed a paramagnetic to ferromagnetic transformation as the temperature was lowered from room temperature to 2K. The ferromagnetic behavior remained even at 10 K. In addition, the Curie temperature for these samples showed linear dependence on the composition. Thus, there is evidence that bulk samples $SmBa_xSr_{1-x}Co_2O_{5+\delta}$ with $0.1 \leq x \leq 0.5$ exhibit strongly activated behavior below their respective Curie temperatures.

ACKNOWLEDGMENTS

One of us Syed N. Qadri is thankful to Prof. John Irvine for his guidance and useful discussions.

[1] A. P. Ramirez, J. Phys., Condens. Matter **9**, 8171 (1997).
[2] P. Schiffer, A. P. Ramirez, W. Bao, and S.-W. Cheong, Phys. Rev. Lett. **75**, 3336 (1995).
[3] A. H. Morrish, *The Physical Principles of Magnetism* (Wiley, New York, 1965).
[4] A. Maignan, C. Martin, D. Pelloquin, N. Nguyen, and B. Raveau, J. Solid State Chem. **142**, 247 (1999).
[5] G. Briceno, H. Chang, X. Sun, P. G. Schultz, and X. D. Xiang, Science **270**, 273 (1995).
[6] S. Yamaguchi, H. Taniguchi, H. Tagagi, T. Arima, and Y. Tokura, J. Phys. Soc. Jpn. **64**, 1885 (1995).
[7] R. Mahendiran and A. K. Raychaudhuri, Phys. Rev. B **54**, 16044 (1996); R. Mahendiran, A. K. Raychaudhuri, A. Chainani, and D. D. Sarma, J. Phys. Condens. Matter **7**, 4561 (1995).
[8] L. Barbey, N. Nguyen, V. Caignaert, M. Hervieu, and B. Raveau, Mat. Res. Bull. **27**, 295 (1992).
[9] L. Barbey, N. Nguyen, V. Caignaert, F. Studer, and B. Raveau, J. Solid State Chem. **112**, 148 (1994).
[10] J. H. Kim, M. Cassidy, J. T. S. Irvine, and J. Bae, J. Electrochem. Soc. **156**, B682 (2009).
[11] A. Jun, J. Kim, J. Shin, and G. Kim, Intl. J. Hydrogen Energ. **37**, 18381 (2012).
[12] A. K. Azad, J. H. Kim, and J. T. S. Irvine, J. Power Sources **196**, 7333 (2011).
[13] A. McKinlay, P. Connor, J. T. S. Irvine, and W. Zhou, J. Phys. Chem. C **111**, 19120 (2007).
[14] A. Maignan, C. Martin, D. Pelloquin, N. Nguyen, and B. Raveau, J. Solid State Chem. **142**, 247 (1999).
[15] J. H. Kim, Y. Kim, P. A. Connor, J. T. S. Irvine, J. Bae, and W. Zhou, J. Power Sources **194**, 704–711 (2009).
[16] J.-H. Kim, F. Prado, and A. Manthiram, J. Electrchem. Soc. **155**, B1023–B1028 (2008).
[17] F. Matsukura, H. Ohno, A. Shen, and Y. Sugawara, Phys. Rev. B **57**, R2037 (1998).
[18] V. A. Kulbachinskii, P. V. Gurin, Yu. A. Danilov, E. I. Malysheva, Y. Horikoshi, and K. Onomitsu, J. of Phys: Conf. Series **61**, 638 (2007).
[19] Q. Gan, R. A. Rao, C. B. Eom, J. L. Garrett, and M. Lee, Appl. Phys. Lett. **72**, 978 (1998).
[20] J. H. Kim, Y. Kim, P. A. Connor, J. T. S. Irvine, J. Bae, and W. Zhou, J. Power Sources **194**, 704–711 (2009).
[21] J.-H. Kim, F. Prado, and A. Manthiram, J. Electrchem. Soc. **155**, B1023–B1028 (2008).